Robotic manipulation project

Binh Nguyen

December 5, 2006

Abstract

This is the draft report for Robotic Manipulation's class project. The chosen project aims to understand and implement Kevin Egan's non-convex constraint[5] as an extended Linear Complementarity problem[6]. This draft contains all the background theories along with analysis needed to complete the project and the implementation progress.

1 Introduction

The main objective of this project is to study Kevin Egan's method[5] and apply it to properly model general 2D polyhedral shapes using LCPs. Due to the limited time, I will just focus on simple test scene which contains a moving sphere and polyhedral obstacles. That will simplify my collision detection. Also, in term of theories and setting LCPs, this simple scene is similar to general polyhedrons - polyhedrons cases. Also, I will not consider friction because it will only complicate implementation. The method extends well to frictional cases.

1.1 Stewart-Trinkle LCP model

Stewart-Trinkle [7] non-penetration constraints maintain a list of active pairs of vertex, edge and try to keep future position of the vertices from penetrating corresponding edges in contact normal direction. This is the same method used in other LCP models which can be studied in [7],[8], [1],[2] .These models linearized contact constraints such that each contact constraint defines a half-space in configuration space. Thus, they can only model locally convex configuration space. This implicit assumption leads to artifacts in simulation. Note that the artifacts only visible in in simulation when two vertices are *close enough*. So, the problems are bearable in some applications.

A simple example that exhibits this artifact is showed in Figure 1 when a point mass approaches a vertex in 2D.

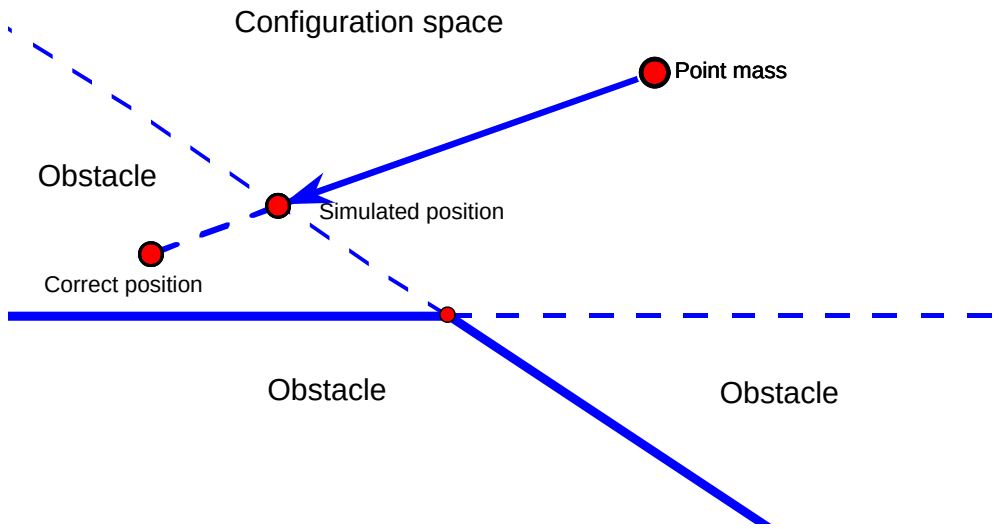

Figure 1: Stewart-Trinkle non-penetration constraints in non-convex configuration space.

The non-penetration constraints in this case are simply the point mass cannot penetrate both edges at the same time.

The point mass cannot penetrate edge 1:

$$0 \leq W_{1n}^T \nu^{l+1} + \frac{\psi_1^l}{h} \quad \perp \quad p_{1n}^{l+1} \geq 0 \tag{1}$$

The point mass cannot penetrate edge 2:

$$0 \leq W_{2n}^T \nu^{l+1} + \frac{\psi_2^l}{h} \quad \perp \quad p_{2n}^{l+1} \geq 0 \tag{2}$$

In which:

ν^{l+1} generalized velocity at the end of time step $[t^l, t^{l+1}]$.

h time step size.

W_{in} normal contact wrench corresponds to edge ith.

p_{in}^{l+1} unknown vector represents magnitude of impulse at contact ith.

ψ_i^l current distance between two contact features of contact ith.

If we define:

$$W_{in}^T \nu^{l+1} + \frac{f_i^l}{h} \triangleq \rho^{l+1} \tag{3}$$

Then ρ_i is the projected distance between corresponding vertex and edge along current normal of contact ith at time t^{l+1}.

We can see that Stewart-Trinkle method limits the simulated possible position of the point mass in the area of $\rho_1 \geq 0 \wedge \rho_2 \geq 0$ which is more restricted than the physically correct one.

We can address this problem by using Kevin Egan's non-convex non-penetration constraint.

1.2 Kevin Egan's model for a locally non-convex corner

Kevin Egan's non-convex non-penetration constraints can model non-convex configuration space with the price of more linear complementarity constraints. In this 2D simple example, the possible position of the point mass is showed in figure 2.

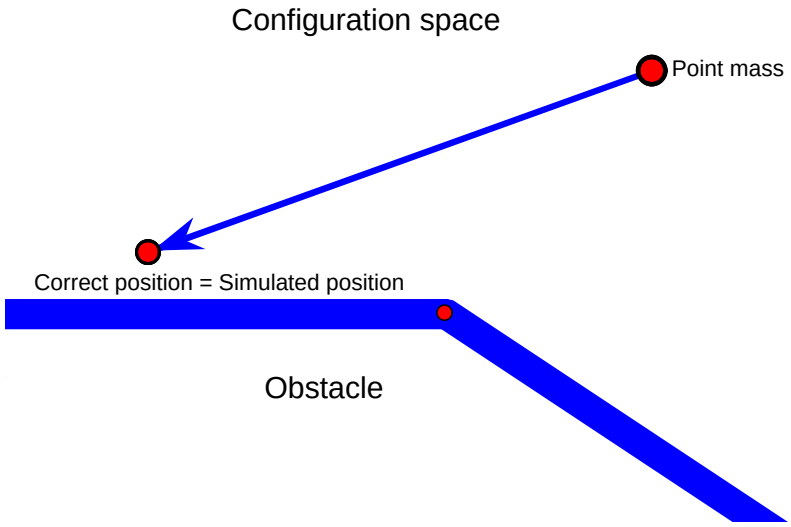

Figure 2: Kevin Egan non-penetration constraints in non-convex configuration space.

Kevin Egan's non-convex model has the ability to *or* the two conditions instead of *and*.So the possible future position of the point mass are $\rho_1 \geq 0 \vee \rho_2 \geq 0$. I will spend the next section on how to use linear complementarity problems to model *or* operator.

1.3 Extending Kevin Egan's model for group of vertices

Figure 3 and 4 show an arbitrary part of a polyhedral shape. In order to model such shape using Kevin Egan's method, we will break the edges into groups follow the rules:

1. If a group contains edges $\{e_{i1}, e_{i2}, ..., e_{ik}\}$ then the configuration space corresponds to that group will be modeled by the set of points that satisfy
$$\rho_{i1} \geq 0 \vee \rho_{i2} \geq 0 \vee ... \vee \ \rho_{ik} \geq 0.$$
In other words, a group that contains more than one edge should form a locally non-convex configuration space or convex obstacle space.

2. There should be no edge belong to two groups. Actually, this rule is just for efficiency purpose. The result should still be the same if we enforce the same constraint more than once.

3. The final configuration space will be modeled by the set of points that satisfy all groups's condition. So the configuration space will be modeled as the area that satisfy: $(\rho_{11} \geq 0 ... \rho_{1k_1} \geq 0) \wedge (\rho_{21} \geq 0 \ ... \rho_{2k_2} \geq 0) ... (\rho_{n1} \geq 0 ... \rho_{nk_p} \geq 0)$.

4. Usually the less number of groups, the better performance. We will see this in later section when we discuss about how to model these conditions.

One thing worth mentioning is that these rules won't guarantee that we will model an *absolutely* accurate configuration space. The accuracy depends on how we break the edges into groups. But this method provide us a much more powerful tool to model locally non-convex space. Also, there are maybe other sets of rules to partition the set of edges but they are beyond the scope of this project.

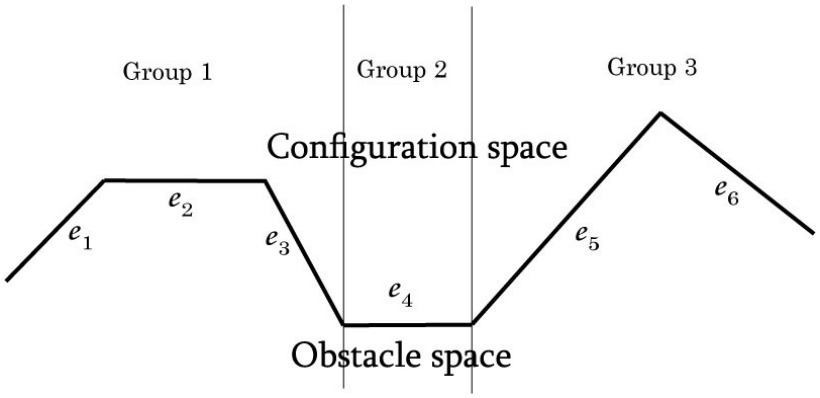

Figure 3: A accurate way to group edges.

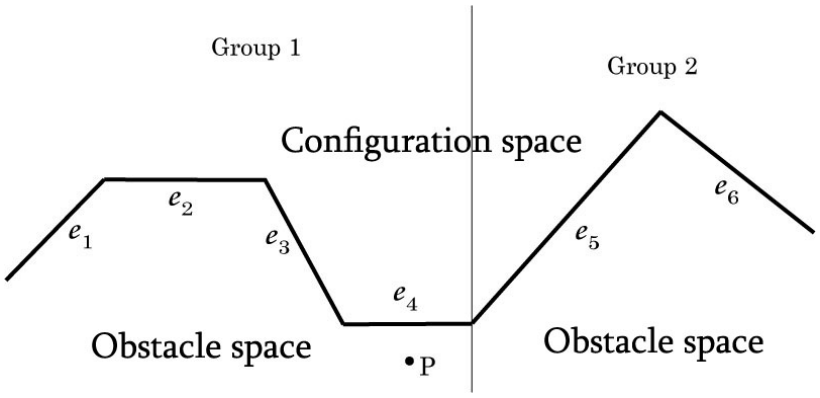

Figure 4: An inaccurate way to group edges.

In figure 4, point P is incorrectly classified as valid because it satisfies condition $\rho_3 \geq 0$. This partition violates rule number 3. If there is an algorithm to partition any polyhedral shapes follow these rules then this set of rules are complete. I leave that algorithm to future work.

Remark I don't have a proof that we will always be able to accurately model any 2D polyhedral obstacle following the rules but I haven't found any counter example.

2 Modeling locally non-convex space using LCP

This section discusses the method to model the *or* operator using LCPs and extend it to model a group of non-convex constraints described in previous section. Kevin Egan reported in [5] two formulations: correct *max* and *summation* with small error. But these two formulations are superseded by a new *diff* formulation which was developed later in a note by Kevin and Jong-Shi Pang[3]. The new formulation has two forms: one simpler but less accurate and one complicated and accurate. For each form, I will first present method to model a simple group with only 2 sides and then extend it to group with n sides.

2.1 Less accurate form

The reason I call this form is less accurate because although it properly models the configuration space described by the group it allows normal impulses exist at any edges in the group even if the distances corresponding to those edges are not zero.

2.1.1 Simple case: group with two sides

If we name the group as $\{e_1, e_2\}$ then the configuration space we want to model is the set of points that satisfy condition:

$$\rho_1 \geq 0 \vee \rho_2 \geq 0 \Leftrightarrow max\{\rho_1, \rho_2\} \geq 0. \tag{4}$$

So if we call normal impulse at edge 1 as p_{1n} then this form's non-penetration constraint is:

$$0 \leq p_{1n} \perp \max\{\rho_1, \rho_2\} \geq 0 \tag{5}$$

$$0 \leq p_{1n} \perp \max\{\rho_1 - \rho_2\} + \rho_2 \geq 0 \tag{6}$$

We will use LCP to model the function $\max\{a, 0\}$ using following observation:

Proposition 2.1 *$c = \max\{a, 0\}$ if and only if $0 \leq c - a \perp c \geq 0$.*

Proof We prove this proposition by checking all possible cases of a's value and make sure in all cases, the results of the two are the same.

- Case 1: $a < 0$:
  $\max\{a, 0\} = 0$ and $c - a > 0 \Rightarrow c = 0$.
- Case 2: $a = 0$:
  $\max\{a, 0\} = 0$ and $c - a = c \Rightarrow c = 0$.
- Case 3: $a > 0$:
  $\max\{a, 0\} = a$ and because $c - a \geq 0 \Rightarrow c > 0 \Rightarrow c = a$ ∎

So the penetration constraint can be written in LCPs form as:

$$\begin{array}{rcrcrcl} 0 & \leq & c_1 - \rho_1 + \rho_2 & \perp & c_1 & \geq & 0 \\ 0 & \leq & c_1 + \rho_2 & \perp & p_{1n}^{l+1} & \geq & 0 \end{array}$$

Similarly, we can write constraint for edge number 2. Then the final non-penetration constraints for the group are:

$$\begin{array}{rcrcrcll} 0 & \leq & c_1 - \rho_1 + \rho_2 & \perp & c_1 & \geq & 0 & (7) \\ 0 & \leq & c_1 + \rho_2 & \perp & p_{1n}^{l+1} & \geq & 0 & (8) \\ 0 & \leq & c_1 + \rho_2 & \perp & p_{2n}^{l+1} & \geq & 0 & (9) \end{array}$$

So the cost for this formulation is one more LCP condition.

2.1.2 Extended case: group with n sides

In this case, the group contains n edges so the configuration space is the set of points that satisfy:

$$\rho_1 \geq 0 \vee ... \vee \rho_n \geq 0 \Leftrightarrow max\{\rho_1, ..., \rho_n\} \geq 0. \quad (10)$$

Then the penetration constraint for edge 1 is:

$$\begin{array}{rcrcrcl} 0 & \leq & p_{1n} & \perp & \max\{\rho_1, \ldots, \rho_n\} & \geq & 0 \\ 0 & \leq & p_{1n} & \perp & \max\{\rho_1, \max\{\rho_2, \ldots, \max\{\rho_{n-1}, \rho_n\} \ldots\}\} & \geq & 0 \end{array}$$

We can use $n-1$ $\max(a, b)$ to get $\max\{\rho_1, \ldots, \rho_n\}$ so the penetration constraints for the group written in LCP form are:

$$
\begin{array}{rcrcll}
0 & \leq & c_2 - \rho_2 + \rho_1 & \perp & c_2 & \geq 0 \\
0 & \leq & c_3 - \rho_3 + c_2 + \rho_1 & \perp & c_3 & \geq 0 \\
 & \cdots & & & & \\
0 & \leq & c_k - \rho_k + c_{k-1} + \cdots + c_2 + \rho_1 & \perp & c_k & \geq 0 \\
 & \cdots & & & & \\
0 & \leq & c_n - \rho_n + c_{n-1} + \cdots + c_2 + \rho_1 & \perp & c_n & \geq 0 \\
0 & \leq & c_2 + c_3 + \cdots + c_n + \rho_1 & \perp & p_{1n}^{l+1} & \geq 0 \\
0 & \leq & c_2 + c_3 + \cdots + c_n + \rho_1 & \perp & p_{2n}^{l+1} & \geq 0 \\
 & \cdots & & & & \\
0 & \leq & c_2 + c_3 + \cdots + c_n + \rho_1 & \perp & p_{nn}^{l+1} & \geq 0
\end{array}
$$

The total number of linear complementarity conditions is $2n-1$ so the price of modeling this non-convex group is $n-1$ conditions.

2.2 Accurate method

The previous formulation could properly model non-convex configuration space but it assumes that normal impulses can exist in all edges in the group. But it doesn't mean that we will always get normal impulse from every edges using previous equation, the LCP solver *may properly* choose the right edge. I present a more complicated formulation described in Kevin Egan and Jong-Shi Pang's note[3] that force normal impulse can only exist at the right edges when the contacts maintained. Again, I will go through simple 2 edges group first, then extend it to many edges group.

2.2.1 Simple case: group with two sides

The main difference is we now force $p_{1n} > 0$ only when $\rho_i = 0$. So the normal impulse at edge 1:

$$p_{1n} > 0 \Leftrightarrow (\max\{\rho_1, \rho_2\} = 0) \wedge (\rho_1 = 0) \tag{11}$$

We model this equation using LCPs using following propositions:

Proposition 2.2
$(\max\{\rho_1, \rho_2\} = 0) \wedge (\rho_1 = 0) \Leftrightarrow (\max\{\rho_1, \rho_2\} = 0) \wedge (\max\{\rho_1, \rho_2\} + |\min\{\rho_1, 0\}| = 0)$.

Proof
We need to prove that when $\max\{\rho_1, \rho_2\} = 0$ then $|\min\{\rho_1, 0\}| = 0 \Leftrightarrow \rho_1 = 0$.

- $\rho_1 = 0 \Rightarrow |\min\{\rho_1, 0\}| = |\min\{0, 0\}| = 0$

- $|\min\{\rho_1, 0\}| = 0 \wedge \max\{\rho_1, \rho_2\} = 0 \Rightarrow \rho_1 = 0$ ∎

We can also model $|\min\{0, 0\}|$ using LCP:

Proposition 2.3
if $|\min\{a, 0\}| = b$ *then* $0 \leq b + a \perp b \geq 0$.

Proof

- Case $a < 0$:$|\min\{a, 0\}| = -a$ and $b + a \geq 0 \Rightarrow b > 0 \Rightarrow a + b = 0 \Rightarrow b = -a$.
- Case $a = 0$:$|\min\{a, 0\}| = 0$ and $0 \leq b \perp b \geq 0 \Rightarrow b = 0$
- Case $a > 0$:$|\min\{a, 0\}| = 0$ and $b \geq 0 \Rightarrow a + b > 0 \Rightarrow b = 0$. ∎

So the final accurate formulation for non-penetration constraint at edge 1 is:

$$\begin{array}{rcrcrcl} 0 & \leq & c_1 - \rho_1 + \rho_2 & \perp & c_1 & \geq & 0 \\ 0 & \leq & g_1 + \rho_1 & \perp & g_1 & \geq & 0 \\ 0 & \leq & c_1 + \rho_2 + g_1 & \perp & p_{1n}^{l+1} & \geq & 0 \\ 0 & \leq & c_1 + \rho_2 & \perp & p & \geq & 0 \end{array}$$

And for edge 2, we need to add two LCPs:

$$\begin{array}{rcrcrcl} 0 & \leq & g_2 + \rho_2 & \perp & g_2 & \geq & 0 \\ 0 & \leq & c_1 + \rho_2 + g_2 & \perp & p_{2n}^{l+1} & \geq & 0 \end{array}$$

So, the cost of accuracy in this formulation is four linear complementarity conditions more than the *non-accurate* one. In which, two conditions are used for moodeling non-convexity, and two conditions for selecting the right edges where collisions happen.

2.2.2 Extended case: group with n sides

In this case, we only need to add n LCPs to force impulse force only exist in constraints correspond to edges that has distance zero. So the final LCPs formulation is:

$$
\begin{array}{rcrcll}
0 & \leq & c_2 - \rho_2 + \rho_1 & \perp & c_2 & \geq 0 \\
0 & \leq & c_3 - \rho_3 + c_2 + \rho_1 & \perp & c_3 & \geq 0 \\
 & \dots & & & & \\
0 & \leq & c_k - \rho_k + c_{k-1} + \cdots + c_2 + \rho_1 & \perp & c_k & \geq 0 \\
 & \dots & & & & \\
0 & \leq & c_n - \rho_n + c_{n-1} + \cdots + c_2 + \rho_1 & \perp & c_n & \geq 0 \\
0 & \leq & g_1 + \rho_1 & \perp & g_1 & \geq 0 \\
0 & \leq & g_2 + \rho_2 & \perp & g_2 & \geq 0 \\
 & \dots & & & & \\
0 & \leq & g_n + \rho_n & \perp & g_n & \geq 0 \\
0 & \leq & g_1 + c_2 + c_3 + \cdots + c_n + \rho_1 & \perp & p_{1n}^{l+1} & \geq 0 \\
0 & \leq & g_2 + c_2 + c_3 + \cdots + c_n + \rho_1 & \perp & p_{2n}^{l+1} & \geq 0 \\
 & \dots & & & & \\
0 & \leq & g_n + c_2 + c_3 + \cdots + c_n + \rho_1 & \perp & p_{nn}^{l+1} & \geq 0 \\
0 & \leq & c_2 + c_3 + \cdots + c_n + \rho_1 & \perp & p & \geq 0
\end{array}
$$

The number of linear complementarity conditions to model a non-convex group of n edges using this accurate formulation is $3n$. In which:

- n to model non-convex configuration space
- n to choose proper edges of contact
- n to model non-penetration constraints

So in general, the price of accuracy in this new formulation is $2n$ more linear complementarity conditions.

3 Implementation

3.1 Putting non-convex constraints in Stewart-Trinkle framework

We know that:

$$\rho_n^{l+1} = \frac{\Psi_n^l}{h} + W_n^{\mathrm{T}} \nu^{l+1} + \frac{\partial \Psi_n^l}{\partial t}$$

So we can express $\rho_i n^{l+1}$ as function of ν^{l+1} to put them in Stewart-Trinkle framework [8]. Below is the complete MLCP formulation I derived using Kevin Egan's accurate formulation

for a non-convex group with n sides. It's easy to extend to many groups by just duplicating complementarity conditions accordingly.

$$
\begin{bmatrix} 0 \\ \zeta_2 \\ \zeta_3 \\ \dots \\ \zeta_n \\ \gamma_1 \\ \gamma_2 \\ \dots \\ \gamma_n \\ \rho_1^{l+1} \\ \rho_2^{l+1} \\ \dots \\ \rho_n^{l+1} \\ \rho^{l+1} \end{bmatrix} = \begin{bmatrix} -M & 0 & \dots & 0 & 0 & \dots & 0 & W_{1n} & \dots & W_{nn} & 0 \\ (W_{1n}^{\mathrm{T}} - W_{2n}^{\mathrm{T}}) & 1 & & & & & & & & & \\ (W_{1n}^{\mathrm{T}} - W_{3n}^{\mathrm{T}}) & 1 & 1 & & & & & & & & \\ \dots & & & & & & & & & & \\ (W_{1n}^{\mathrm{T}} - W_{nn}^{\mathrm{T}}) & 1 & \dots & 1 & & & & & & & \\ W_{1n}^{\mathrm{T}} & 0 & \dots & 0 & 1 & & & & & & \\ W_{2n}^{\mathrm{T}} & 0 & \dots & 0 & 0 & 1 & & & & & \\ \dots & & & & & & & & & & \\ W_{nn}^{\mathrm{T}} & 0 & \dots & 0 & 0 & \dots & 1 & & & & \\ W_{1n}^{\mathrm{T}} & 1 & \dots & 1 & & & & & & & \\ W_{2n}^{\mathrm{T}} & 1 & \dots & 1 & 0 & 1 & & & & & \\ \dots & & & & & & & & & & \\ W_{nn}^{\mathrm{T}} & 1 & \dots & 1 & 0 & \dots & 1 & & & & \\ W_{1n}^{\mathrm{T}} & 1 & \dots & 1 & & & & & & & \end{bmatrix} \begin{bmatrix} \nu^{l+1} \\ c_2 \\ c_3 \\ \dots \\ c_n \\ g_1 \\ g_2 \\ \dots \\ g_n \\ p_{1n}^{l+1} \\ p_{2n}^{l+1} \\ \dots \\ p_{nn}^{l+1} \\ p^{l+1} \end{bmatrix}
$$

$$
+ \begin{bmatrix} M\nu^l + p_{ext}^l \\ \frac{\Psi_{1n}^l}{h} + \frac{\partial \Psi_{1n}^l}{\partial t} - \frac{\Psi_{2n}^l}{h} + \frac{\partial \Psi_{2n}^l}{\partial t} \\ \frac{\Psi_{1n}^l}{h} + \frac{\partial \Psi_{1n}^l}{\partial t} - \frac{\Psi_{3n}^l}{h} + \frac{\partial \Psi_{3n}^l}{\partial t} \\ \dots \\ \frac{\Psi_{1n}^l}{h} + \frac{\partial \Psi_{1n}^l}{\partial t} - \frac{\Psi_{nn}^l}{h} + \frac{\partial \Psi_{nn}^l}{\partial t} \\ \frac{\Psi_{1n}^l}{h} + \frac{\partial \Psi_{1n}^l}{\partial t} \\ \frac{\Psi_{2n}^l}{h} + \frac{\partial \Psi_{2n}^l}{\partial t} \\ \dots \\ \frac{\Psi_{nn}^l}{h} + \frac{\partial \Psi_{nn}^l}{\partial t} \\ \frac{\Psi_{1n}^l}{h} + \frac{\partial \Psi_{1n}^l}{\partial t} \\ \frac{\Psi_{2n}^l}{h} + \frac{\partial \Psi_{2n}^l}{\partial t} \\ \dots \\ \frac{\Psi_{nn}^l}{h} + \frac{\partial \Psi_{nn}^l}{\partial t} \\ \frac{\Psi_{1n}^l}{h} + \frac{\partial \Psi_{1n}^l}{\partial t} \end{bmatrix}; \quad \begin{bmatrix} \zeta_2 \\ \zeta_3 \\ \dots \\ \zeta_n \\ \gamma_1 \\ \gamma_2 \\ \dots \\ \gamma_n \\ \rho_1^{l+1} \\ \rho_2^{l+1} \\ \dots \\ \rho_n^{l+1} \\ \rho^{l+1} \end{bmatrix} \perp \begin{bmatrix} c_2 \\ c_3 \\ \dots \\ c_n \\ g_1 \\ g_2 \\ \dots \\ g_n \\ p_{1n}^{l+1} \\ p_{2n}^{l+1} \\ \dots \\ p_{nn}^{l+1} \\ p^{l+1} \end{bmatrix} \tag{12}
$$

The big matrix we usually called B for one n sides group is $3n + 2 \times 3n + 2$.

3.2 Project's implementation

I have finished the coding part to test these new formulations. The demo program contains three time-steppers:

- Original Stewart-Trinkle time-stepper

- Kevin Egan's simple non-convex formulation
- Kevin Egan's accurate non-convex formulation

Below is a screenshot of the demo running with simple non-convex formulation:

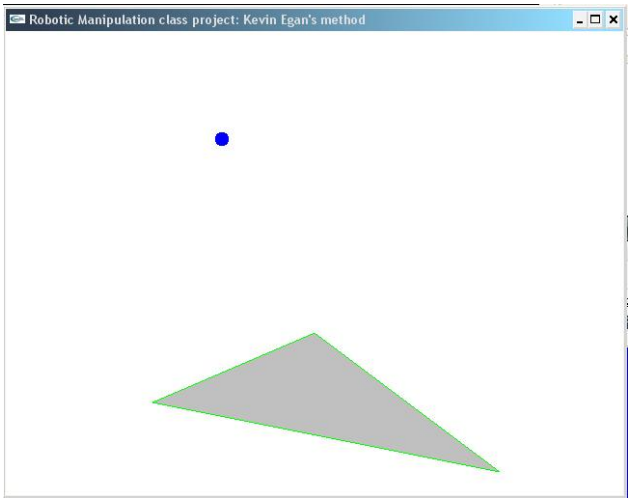

Here are the list of some features built in this demo:

- Read geometry from external file
- Allow simple user interaction
- Work with moving particle and static polyhedral shapes

In short, it can be used to test Kevin Egan's formulations.

4 Some interesting results

In this section, I will provide some interesting results from implementing Kevin Egan's formulation.

4.1 Simple formulation

The demo program shows that the method works as expected. We really get a non-convex configuration space as the particle could travel pass the virtual edge smoothly. But once in contact with the edges, the particle will automatically move along the edge as we allow normal impulses at all edges. This effect is showed below:

The particle can travel through virtual edge to get in contact with the edges.

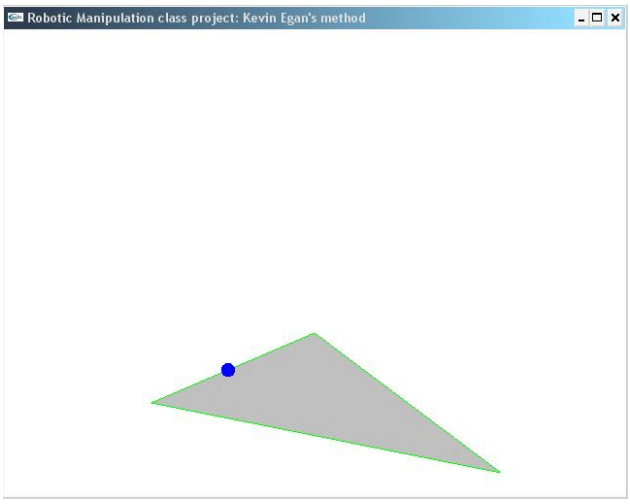

But once in contact, it will move along the edge. The direction of the move depends on the edges's normal.

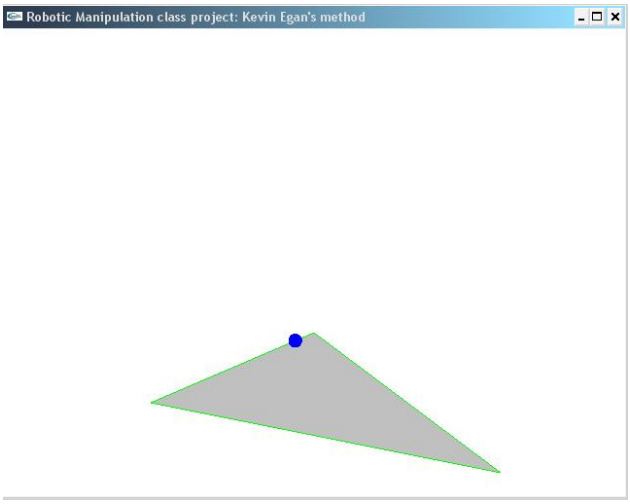

It shows that we can overcome the *virtual edge*'s artifact caused by convex assumption of original Stewart-Trinkle time stepper but it leads to another problem. Actually, depend on applications, this problem can be treated in some ways. One way of which is checking p_n^{l+1} for in contact event. If it's in contact then switch to original Stewart-Trinkle time stepper.

4.2 Accurate formulation

After a long time trying to implement this more complicated formulation, I found out that there is one linear complementarity condition that leads to singularity in our big matrix. And this singularity make my LCP's solver, *PATH* [4], fails (crashed) after some time steps.

That condition is:

$$0 \quad \leq \quad c_2 + c_3 + \cdots + c_n + \rho_1 \quad \perp \quad p \quad \geq \quad 0$$

In which, p is just a dummy variable and no other conditions need p. That leads to a full column of 0 in the big matrix.

I have tried to introduce an small ϵ amount of p in the left hand side but it makes the simulation unstable. Maybe there is other way of dealing with it but in a short time, I could not think of any.

Below is the screen-shot that shows the big matrix in simulation:

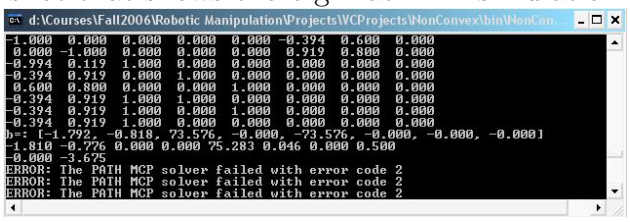

4.3 Can Kevin Egan's method model *precisely* all planar obstacle?

Right now I don't have an absolute answer for polyhedron vs polyhedral case but the answer for the case with very simple implicit object: circle vs polyhedron is **NO**.

Below is the case where Kevin Egan's method doesn't work with circle:

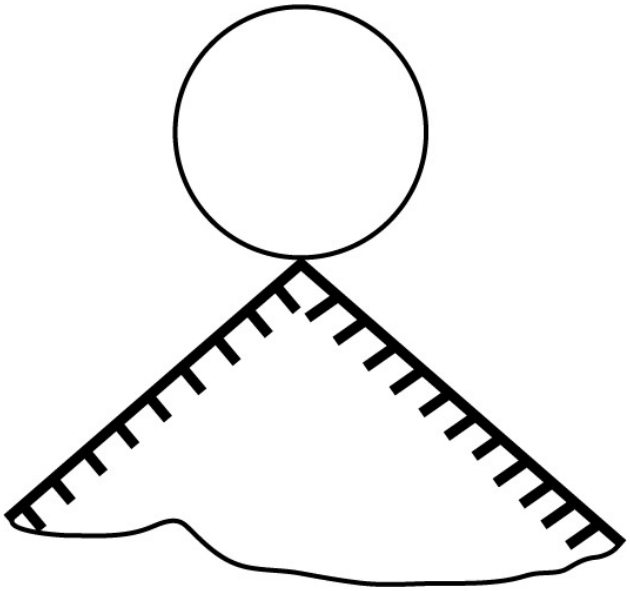

This is completely valid configuration but Kevin Egan's method will report it as invalid because both distances are negative.

5 Future works

There are some areas we can explore in the future:

- Using topology information of a polyhedral shape in convex formulation.
- Advance into 3D.
- Work with implicit surfaces by discretizing the surfaces on the fly and model it with convex/non-convex obstacle.
- Find an algorithm to partition arbitrary polyhedral shape into groups.
- Fix the accurate formulation

References

[1] M. Anitescu and F.A. Potra. A time-stepping method for stiff multibody dynamics with contact and friction. *International Journal for Numerical Methods in Engineering*, 55: 753–784, 2002.

[2] D. Baraff. Issues in computing contact forces for non-penetrating rigid bodies. *Algorithmica*, pages 292–352, October 1993.

[3] Kevin Egan. More thoughts on nonconvex constraints. 2004.

[4] Michael C. Ferris and Todd S. Munson. Path cp solver. URL http://www.cs.wisc.edu/cpnet/cpnetsoftware/. 2002.

[5] S. Berard K.T. Egan and J.C. Trinkle. Modeling nonconvex constraints using linear complementarity. Technical Report 03-13, 2004.

[6] Katta G. Murty. *Linear Complementarity, Linear and Nonlinear Programming Internet Edition*. Helderman-Verlag, 1988. URL http://ioe.engin.umich.edu/people/fac/books/murty/linear_complementarity_webbook/.

[7] D.E. Stewart and J.C. Trinkle. An implicit time-stepping scheme for rigid body dynamics with inelastic collisions and coulomb friction. *Int'l Jrnl. of Numerical Methods in Engineering*, pages 2673–2691, 1996.

[8] D.E. Stewart and J.C. Trinkle. An implicit time-stepping scheme for rigid body dynamics with inelastic collisions and coulomb friction. *International Journal of Numerical Methods in Engineering*, 39:2673–2691, 1996.